CHAPTER IV

RESULTS AND DISCUSSIONS

In this chapter, results and discussions were divided into 4 sections. In the first section, the investigation and characterization of the treated CNTs was reported and discussed. The second was related to examination of characterized TNTs and rice-shaped TiO_2. The third involved with preparation and characterization the TNTS and CNTs composites. At the end, the efficiency of DSSCs was investigated and discussed.

4.1 Investigation and characterization of modified CNTs

Due to the poor dispersability of virgin CNTs particles they were treated by ultrasonication in HNO_3 solution to form some functional groups on their surface. Figure 4.1 shows that FT-IR spectra of sonicate virgin CNTs and treated CNTs. The peak of carboxylic acid group, -C=O, was observed at 1710 cm^{-1} and the peak of broad OH vibration at 3400 cm^{-1}. So, the existence of carboxylic acid group on the surface of treated CNTs was confirmed.

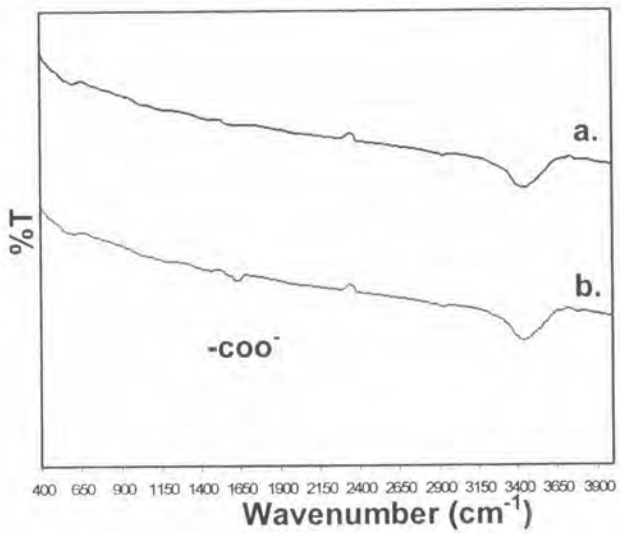

Figure 4.1 FT-IR analysis of a) virgin CNTs b) treated CNTs(TrCNTs).

The ability of suspension of CNTs particles would refer to uniformity of CNTs distribution in a composite material (Park et al., 2007; Bikiaris et al., 2007). Thus, the suspensibility of virgin CNTs and TrCNTs were investigated. Both types of particles were sonicated in Terpineol solution for 30 min. As noticed in Figure 4.2, seven days after the operation, virgin CNTs settled down to the bottom of the vessel while the treated CNTs (TrCNTs) particles were found suspending in the Terpineol.

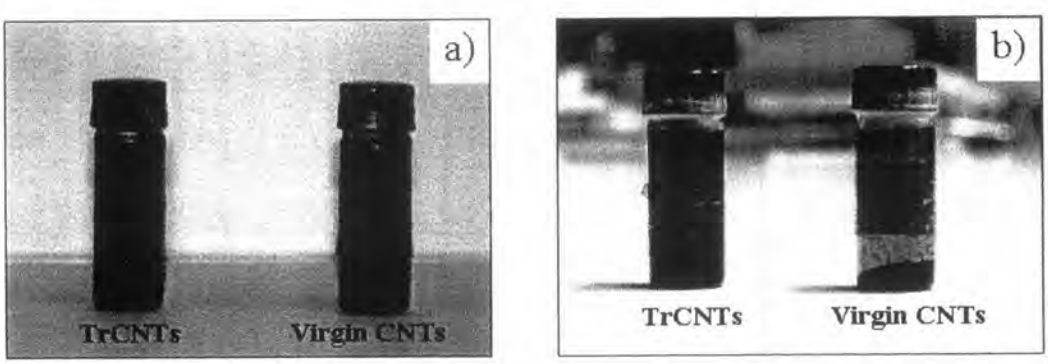

Figure 4.2 Suspension of CNTs a) 0 day b) 7day.

According to the existence of carboxylic group on the surface of TrCNTS, It could be implied that the TrCNTs could be steadily dispersed in the Terpineol. Since the carboxylic –COOH located on the surface could enhanced their polar properties and prevent particles from agglomeration. There is also a previous repeat that such treated CNTs could preferably attach dye molecule (Lee and Yoo, 2005). Therefore, it could be supposed that the treated CNTs would be suitable for application of dye-sensitized solar cell.

4.2 Examination of TNTs and rice-shaped TiO_2

To find the suitable condition for preparation of CNTs and titania derivatives composites, TNTs and rice-shaped TiO_2 were taken into account. Because there are some reports showing that there materials are promising for DSSCs applications. It showed to be noted that, TNTs could be obtained by hydrothermal treatment of rutile TiO_2 (Viriya-empikul et al., 2008). Figure 4.3, reveal typical micrograph of rutile TiO_2 particle with average diameter was around 500-1000 nm.

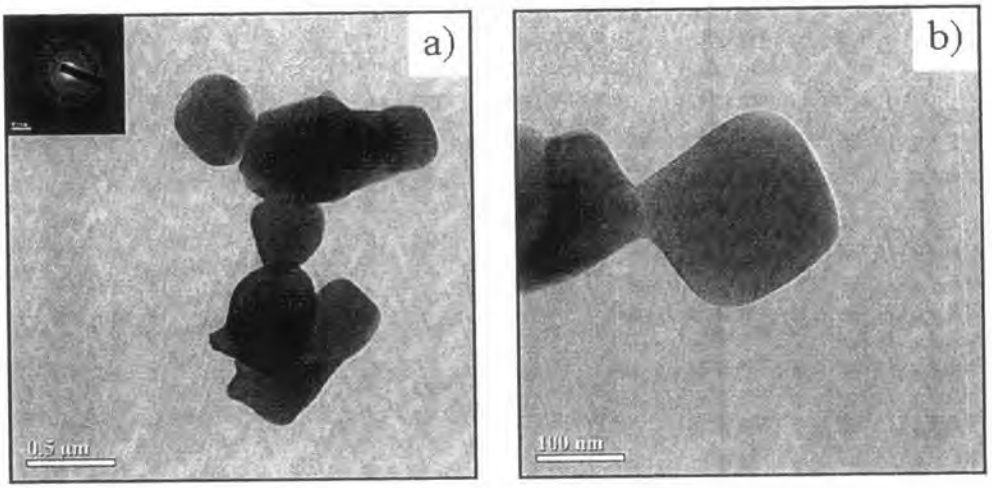

Figure 4.3 TEM image of rutile TiO_2 a) low magnification image b) high magnification image.

Based on the previous work reported by Kasuga (2006), TiO_2 crystals become amorphous because the Ti-O bond is broken and Ti-O-Na or Ti-OH bonds are arbitrarily formed following treatment in aqueous NaOH, and titanate nanotubes are generated after the treatment of TiO_2 crystals in acidic solution/water. Their average diameter was around 7 nm with an average aspect ratio of 14. Based on adsorption analysis, the BET surface area was measured as 134 m^2/g. Moreover, XRD results, shown in Figure 4.5 b), reveal that TNTs shown lacking of phase crystalline.

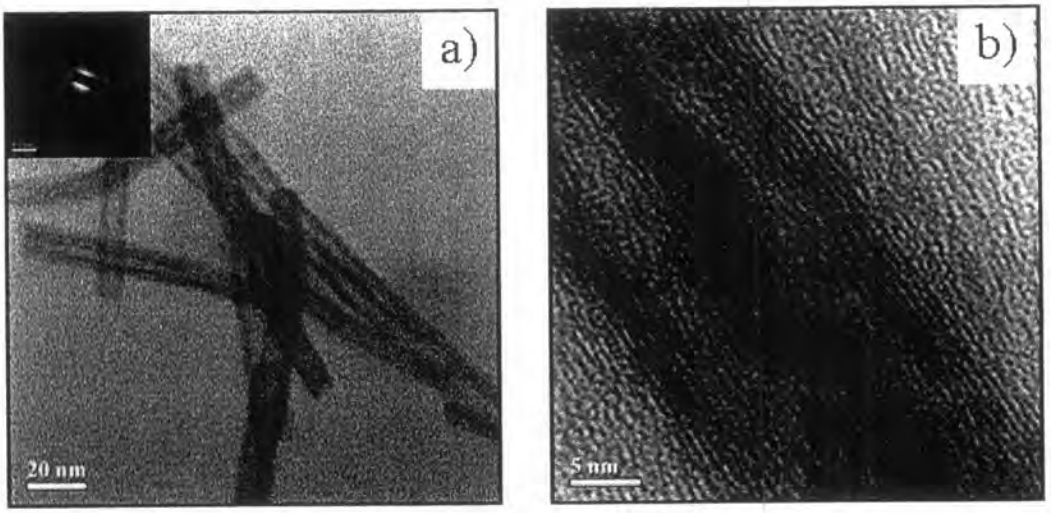

Figure 4.4 TEM image of TNTs fabrication by the first hydrothermal treatment a) low magnification image b) high magnification image.

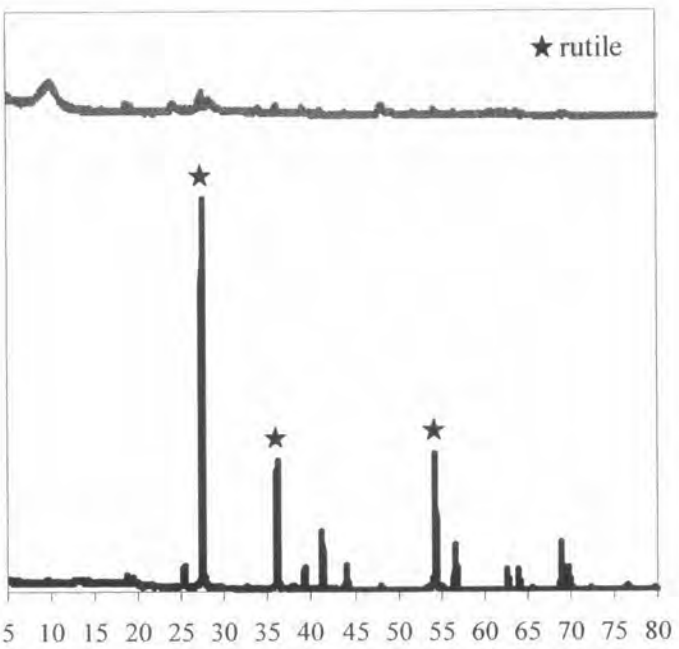

Figure 4.5 XRD spectra of a) rutile TiO_2 commercial, b) TNTs.

Under a certain condition, TNTs could be obtained from a single step hydrothermal process. Then, TNTs were used as precursors to investigate the procedures of secondary treatment with different types of media and incubation time. Sodium Hydroxide solution (NaOH), water with oxygen anion, and deionized water were employed as treatment media for the preparation of anatase titania in the secondary treatment.

10-M NaOH solution was first employed as media for secondary hydrothermal of TNTs in the same Teflon autoclave for 72 hr. TEM image in Figure 4.6 a. and b. reveal morphology and crystal structure of TNTs fabricated in the secondary treatment.

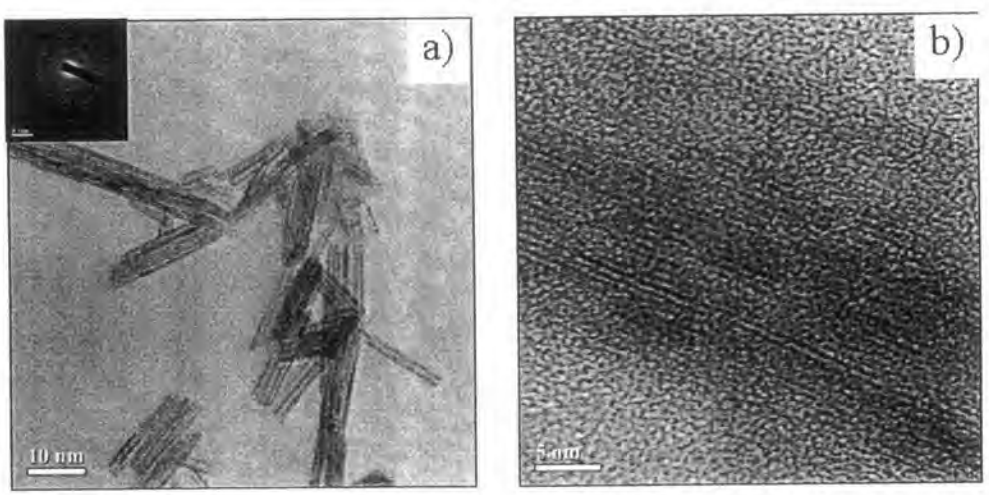

Figure 4.6 TEM images of the secondary hydrothermal TNTs in NaOH a) low magnification image b) high magnification image.

According to XRD results shown in Figure 4.7 secondary hydrothermal TNTs in NaOH-10 M, exhibit distinctive difference in XRD spectra of TNTs in Figure 4.5 b. They showed both amorphous phase. These could be explained that Na^+ regularly played a role to break the bond of Ti-O and Ti-O-Na or Ti-OH bonds are arbitrarily formed following treatment in aqueous NaOH, and titanate nanotubes are generated after the treatment of TiO_2 crystals in acidic solution/water.

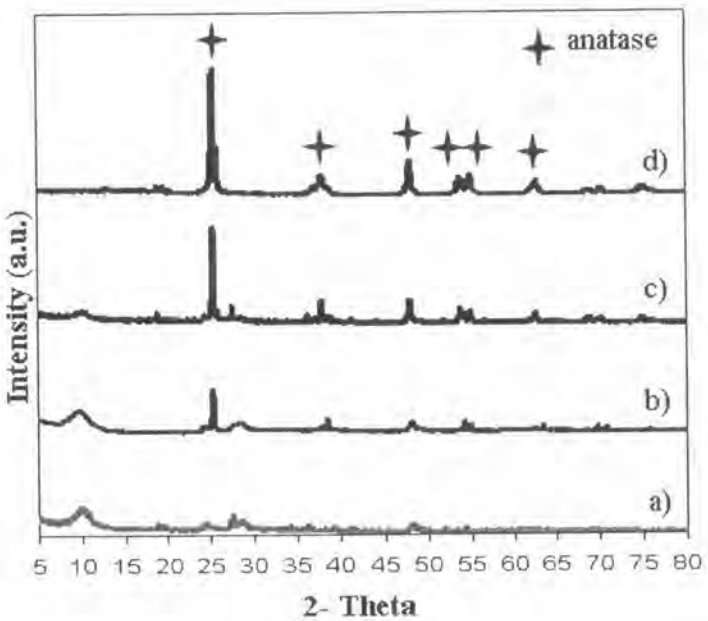

Figure 4.7 XRD spectra of a) secondary hydrothermal TNTs in NaOH

b) secondary hydrothermal TNTs in water with oxygen anion

c) secondary hydrothermal TNTs in deionized water and

d) commercial anatase TiO_2.

Next, media without Sodium Cation (Na^+) was further applied. Water with oxygen anion was employed as treatment media in the secondary treatment. The product morphology could be observed in Figure 4.8.

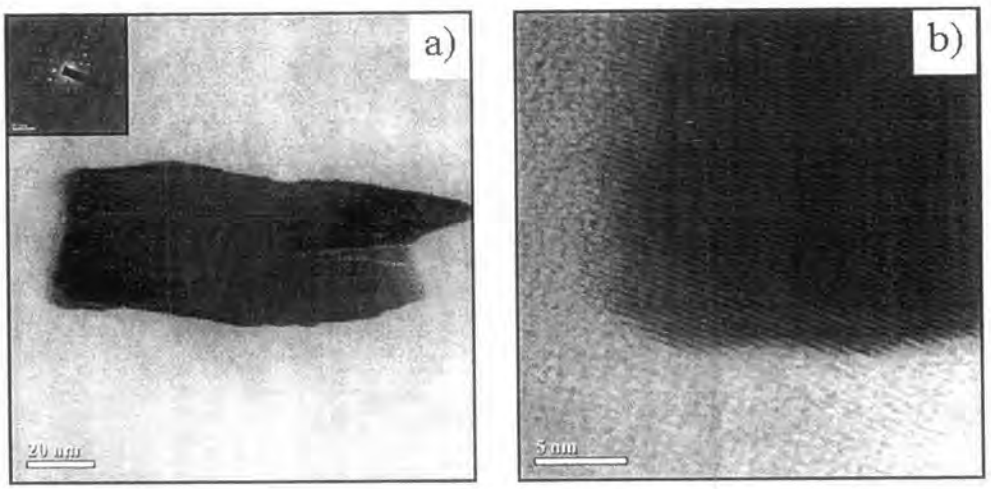

Figure 4.8 TEM images of secondary hydrothermal TNTs in water with oxygen anion a) low magnification image b) high magnification image.

Also, from XRD results in Figure 4.7c), comparatively intensive peak of anatase TiO_2 could be observed in the specimen of secondary treatment of TNTs when compared with the product fabricated in NaOH solution (Figure 4.7b).

Deionized water was the last media. After undergoing hydrothermal treatment in deionized water, the TNTs were transformed to rice-shaped TiO_2 with minor axis diameter of 51 nm and BET area of 80 m^2/g. The distinctive change in their morphology is revealed in Figure 4.9 a. and 4.9 b.

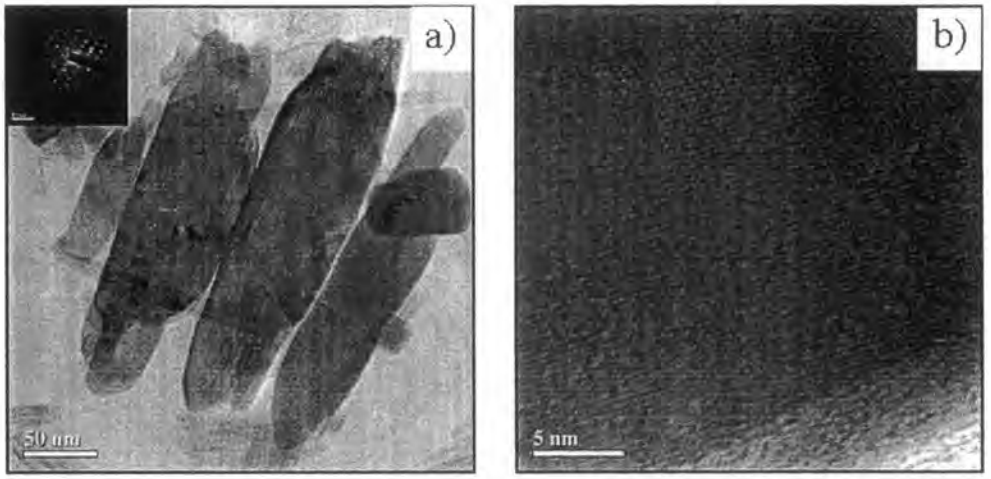

Figure 4.9 TEM images of secondary hydrothermal TNTs in deionized water a) low magnification image b) high magnification image.

From SAED analyses, it was confirmed that the starting rutile titania and the synthesized rice-shaped titania exhibited clear crystallinity while the TNTs were amorphous. The d-spacing within the crystal lattice of the rice-shaped titania crystals was 0.35 and 0.24 nm with corresponding to the 101 and 103 planes, respectively. Moreover, TEM image also showed some of TNTs which could not be absolutely converted to rice-shaped TiO_2 one. The (rice-shaped TiO_2 is significantly bigger in size than the TNTs. This result is attributed to the agglomeration of TNTs during being attacked by water molecules under the high pressure and temperature condition. It is worth noting that at temperature 150 ^{o}C, water in the autoclave reactor was still at its saturated state. The mild condition in the second treatment implies that the drastic change in size, surface area and morphology as well as phase of the titania were possibly attributed to the phase transformation and crystallization of titania. The crystallinity of the raw material and the prepared nanostructures was reconfirmed by the analytical result of X-ray diffracto-photometry as shown in Figure. 4.7. With the second step of hydrothermal treatment with deionized water, the TNTs was further

transformed to rice-shaped TiO_2 with recovered crystallinity. It was reported that, because of lack of crystallinity, TNTs possess low stability and could be easily transformed to another structure with higher stability by hydrothermal treatment in an autoclave. In this experiment, they preferred to change themselves to anatase phase. The rice-shaped TiO_2 exhibited an remarkably smaller aspect ratio of ca. 5.

The product from deionized water showed the most distinguish peak of anatase which were useful for DSSCs. It was used as media for investigation the effect of time to phase of product. The incubation time were investigated at 12, 48 and 72 hr. It started with 12 hr hydrothermal incubation time treatment. TEM images in Figure 4.10 a. and b. presented a lot of TNTs and some of processing formation rice shape. From XRD, this product showed crystallinity like TNTs formation.

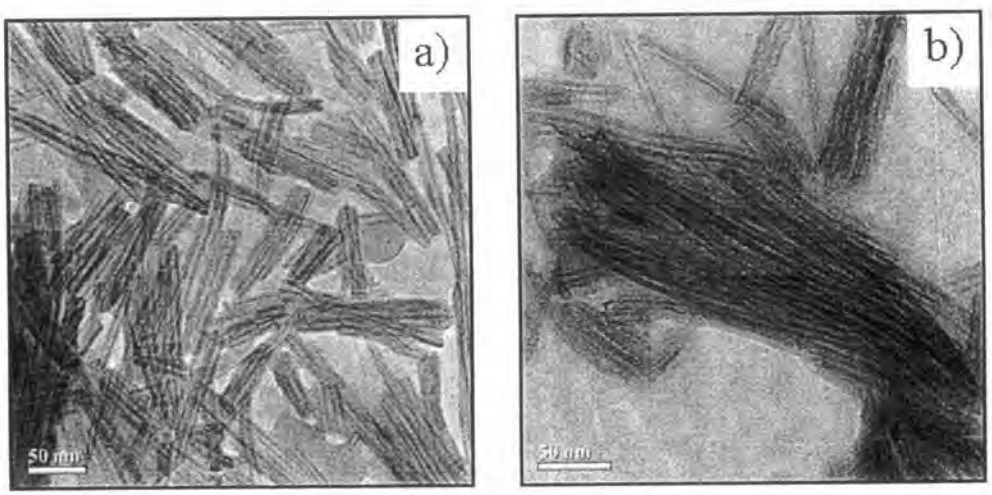

Figure 4.10 TEM images of secondary hydrothermal TNTs in deionized water for 12 hr a) low magnification image b) high magnification image.

The 48 hr incubation time was investigated. TEM images in Figure 4.11 reveal some of (rice-shape) TiO_2 and the processing of formation. This process incubation time could provide some of anatase particles which showed in Figure 4.12 c) The 48 hr incubation time products was compared their phase crystallinity with 72 hr in Figure 2.12d). The 72 hr incubation time showed outstanding phase of anatase compared with commercial anatase in Figure 4.2e). From TEM images in Figure 4.9 showed the form of producing in rice-shape. So, these products were called rice shaped TiO_2. The 72 hr incubation time in autoclave was obtained appropriate energy and pressure to molecule of TNTs in order to transform their non-crystalline to crystalline structure.

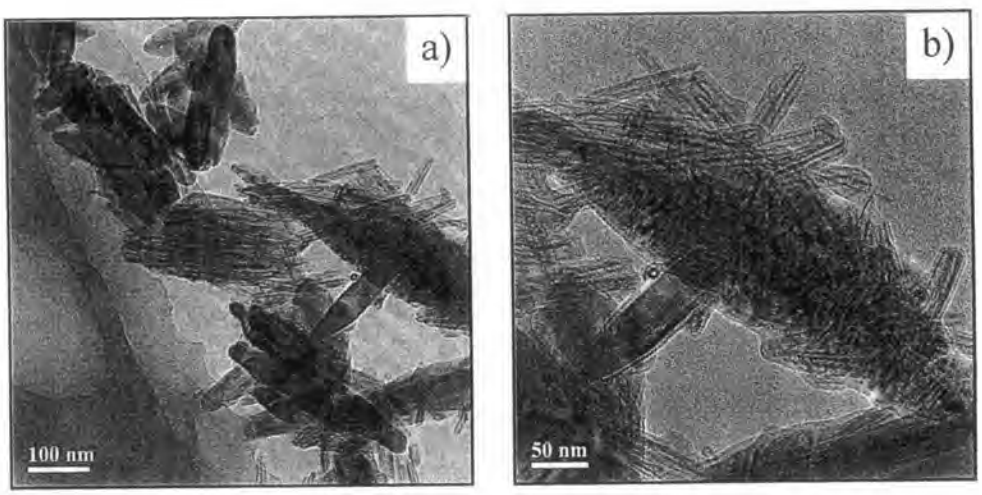

Figure 4.11 TEM images of secondary hydrothermal TNTs in deionized water for 48 hr a) low magnification image b) high magnification image.

The effect of time related to pressure inside autoclave. The 72 hr incubation could be provided the appropriated pressure to prepare anatase phase in the form of rice-shaped TiO_2.

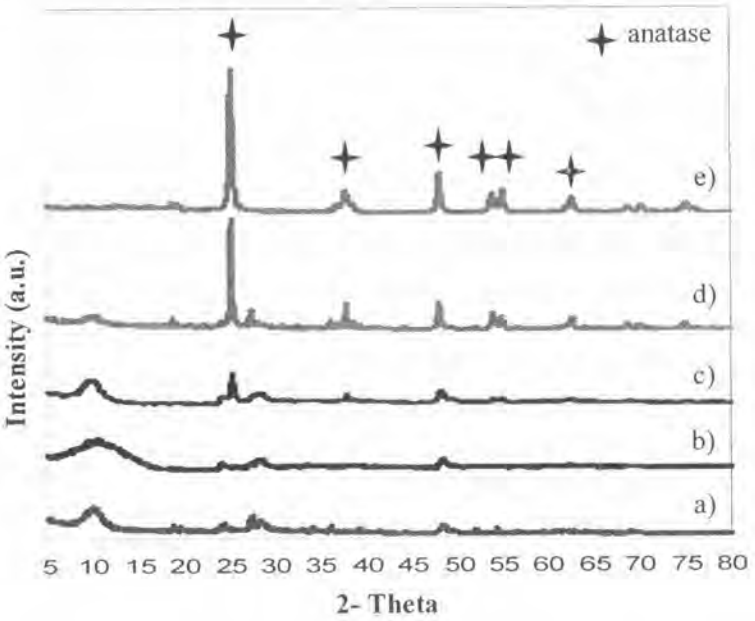

Figure 4.12 XRD spectra of a)primary TNTs, b) secondary hydrothermal at 12 hr a) secondary hydrothermal at 48 hr d) secondary hydrothermal at 72 hr.

Therefore, the certain condition for preparing of anatase by secondary treatment TNTs was 72 hr incubation and deionized water worked as media.

4.3 Preparation of the composite

The most suitable condition for the preparation of TNTs and rice-shaped TiO_2 was used to prepare the composite material of CNTs and titanium derivatives. Two composites structure of CNT-TNT composite and TrCNT-TNT composite were produced *via* first step hydrothermal of TNTs. Firstly, either CNTs and treated CNTs (TrCNTs) would be added to titanium dioxide (TiO_2) media with NaOH solution. The well dispersed mixture was obtained by the aide of ultrasonication. The secondary step hydrothermal treatment would be done in order to prepare the rice-shaped TiO_2 particles which would be employed for production of CNT - rice-shaped TiO_2 composite and TrCNT - rice-shaped TiO_2 composite. Either CNTs or TrCNTs would be combined with TNTs as precursors for hydrothermal process using deionized water. Afterward, the composite were characterized by TEM XRD and BET, as appear in Figures 4.13, 4.14, 4.15, 4.16, 4.17 and Table 4.1.

Figure 4.13 TEM image of CNT-TNT composite.

Figure 4.14 TEM image of TrCNT-TNT composite

Referring to Figures 4.13 and 4.14, hollow shape of TNTs with an average diameter of about 5-20 nm could be noticed. The tube shape composite material is expected to provide the rough surface thin film, promoting absorption rate for the remediation of dye components (Ong et al., 2007 and Bwana, 2008). The phase crystallinity of CNT-TNT composite and TrCNT-TNT composite were shown by XRD (Figure 4.17). In brief, CNT-TNT and TrCNT-TNT composite exhibit the same amorphous phase as that of TNTs. There is a report that high aspect ratio of TNTs would enhance electron transport and avoid charge recombination of DSSCs (Hsiao et al., 2007)

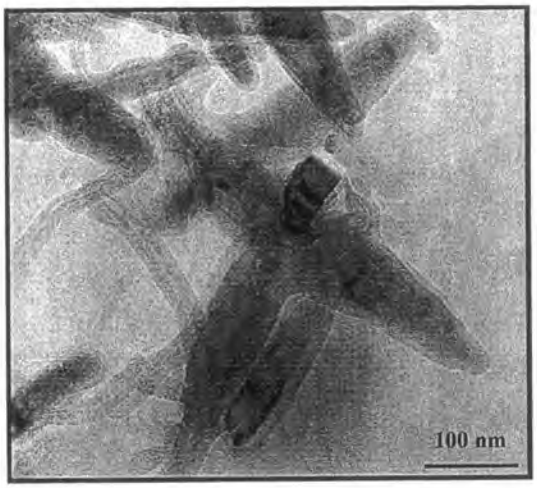

Figure 4.15 TEM image of CNT- rice-shaped TiO_2 composite.

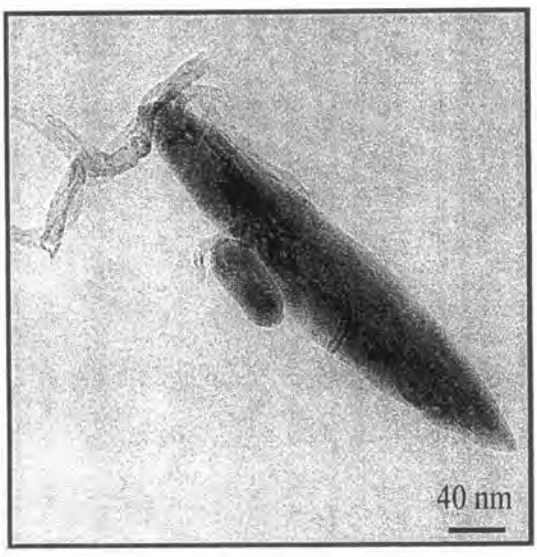

Figure 4.16 TEM image of composite TrCNT- rice-shaped TiO_2 composite.

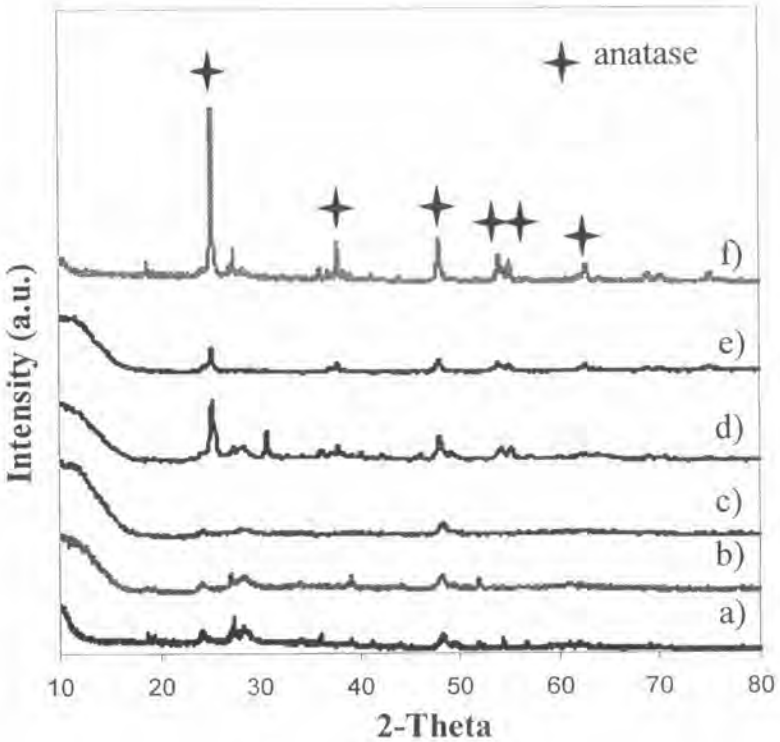

Figure 4.17 XRD spectra of a) TNTs, b) CNT-TNT composite c) TrCNT-TNT composite, d) CNT - rice-shaped TiO_2 composite e) TrCNT - rice-shaped TiO_2 composite and f) rice-shaped TiO_2.

The morphology of the composite CNT - rice-shaped TiO_2 composite and TrCNTs - rice-shaped TiO_2 composite appeared in the form of rice shape along with carbon nanotubes as shown in Figures 4.15 and 4.16, respectively. Phase of these two composites was characterized and shown in Figure 4.17 d) and e). Based on XRD analysis shown in Figure 4.17, CNT - rice-shaped TiO_2 composite and TrCNT - rice-shaped TiO_2 composite exhibit small peak of anatase and non-crystalline phase indicate that TNTs could not be completely converted into rice shape anatase form.

Table 4.1 BET analysis of surface area and pore volume of the composites.

Composites	A_s (m^2/g)	V_m (m^3/g)
CNT-TNT	172.55	39.65
TrCNT-TNT	196.19	45.08
CNT- rice shaped TiO_2	90.45	21.69
TrCNT- rice-shaped TiO_2	97.21	22.33

From BET analysis, pore volume(V_m) was correlated to surface area. TrCNT-TNT composite was showed maximum surface area at 196.19 m^2/g. TrCNT-TNT composite tends to provide the higher surface area compared with CNT-TNT composite; likewise, TrCNT - rice-shaped TiO_2 composite possesses more surface area than CNT - rice-shaped TiO_2 composite. The larger surface area of TrCNTs composite could be explained by the higher dispersability leaded to the prevention of agglomeration. Moreover, the rice-shaped TiO_2, TrCNT-rice-shaped TiO_2 , CNT - rice-shaped TiO_2, TrCNT-TNT and CNT-TNT composite tends .to provide less surface area compared with hollow-shape TNTs. It should be noted that the specific surface area of the synthesized composite material may related to the energy conversion efficiency of DSSCs.

4.4 Effects of the titanium derivatives and their composites to the DSSCs eficiency

The screen printed TiO_2 film was sintered at 500 °C to remove organic additives. The surface morphology of TNTs and rice-shaped TiO_2 were observed by FESEM as shown in Figures 4.18 and 4.19, respectively.

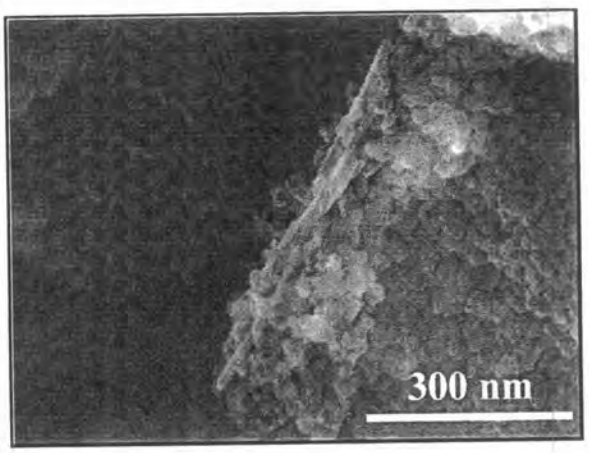

Figure 4.18 FESEM image of TiO_2 film containing 0.21 %wt TNTs.

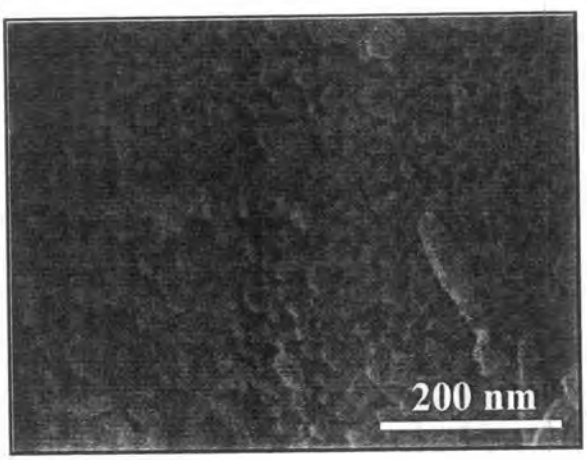

Figure 4.19 FESEM image of TiO_2 film containing 0.21 %wt rice-shaped TiO_2.

FESEM show the presence of TNTs and rice-shaped TiO_2 in TiO_2 film indicated that the sintering temperature (500 ^{o}C) does not affect the material structure. The existence of TNTs and rice-shaped TiO_2 may lead to the rough surface; consequently, would enhance the absorption in dye remediation process (Bwana, 2008; Ong et al., 2007).

The effect of the quantity of synthetic TiO_2 (TNTs, rice-shaped TiO_2 and the prepared composites) at 0, 0.21, 1.06, 2.1 and 21 %wt as the additives in the commercial anatase TiO_2 were investigated. The DSSCs efficiency with respect to TNTs, CNT-TNT composite and TrCNT-TNT composite were shown in Figures 4.20, 4.21 and 4.22, respectively. The equations applied in the calculation of efficiency were illustrated as follows;

$$\%\eta = \frac{I_{sc}V_{oc}FF}{P_s},$$

$$FF = \frac{V_m I_m}{V_{oc} I_{sc}}$$

where I_{sc}, V_{oc}, FF, P_s, V_m, and I_m were short circuit current, open circuit voltage, fill factor, standard power of incident light, maximum voltage and maximum current, respectively.

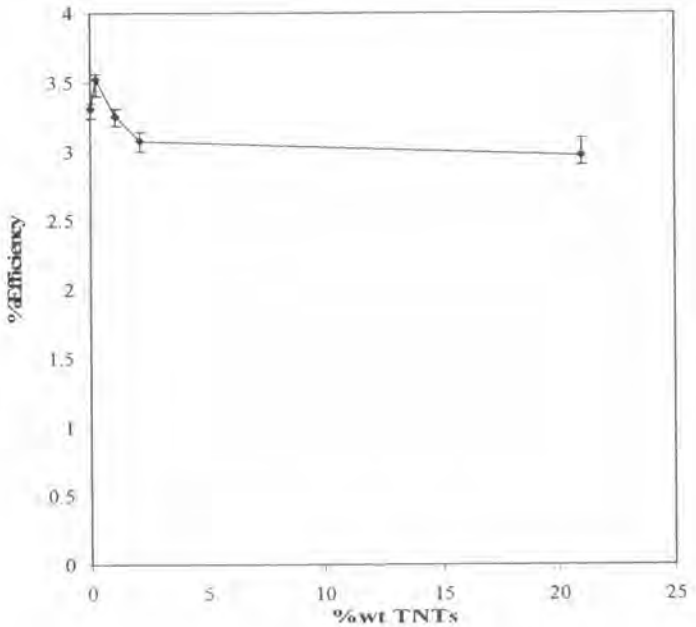

Figure 4.20 Dependence of DSSCs efficiency on amount of TNTs.

From Figure 4.20, the efficiency of DSSCs based on TiO_2 film as working electrode increased from 3.31% to 3.53% (increases 6.65%). The hollow-structure TNTs result in the increase of porous structure to the accommodation of the dye absorption. Both TNTs and anatase TiO2 are wide band gap semiconductor with the gap approximate at 3.30 eV(Gao et al., 2008) and 3.20 eV, respectively. The increase of band gap could reduce charge recombination. Moreover, TNTs show high aspect ratio of ca.80 which would provide an advantage for electron transportation of electrode and avoid charge recombination (Hsiao et al., 2007). On the other hand, the graph show decrease of efficiency after addition of 0.21 %wt of TNTs. Because the lower BET surface area of TNTs (134 m^2/g) would oppositely result in less active area for dye adsorption when compared with anatase TiO_2 (272 m^2/g). The increasing the amount of TNTs would effect to reflection of sunlight to solar cell that reduce the exitation energy to dye.

Next, the effect of CNT-TNT composition on DSSCs efficiency was investigated. The correlations between CNT-TNT composite and DSSCs efficiencies were showed in Figure 4.21.

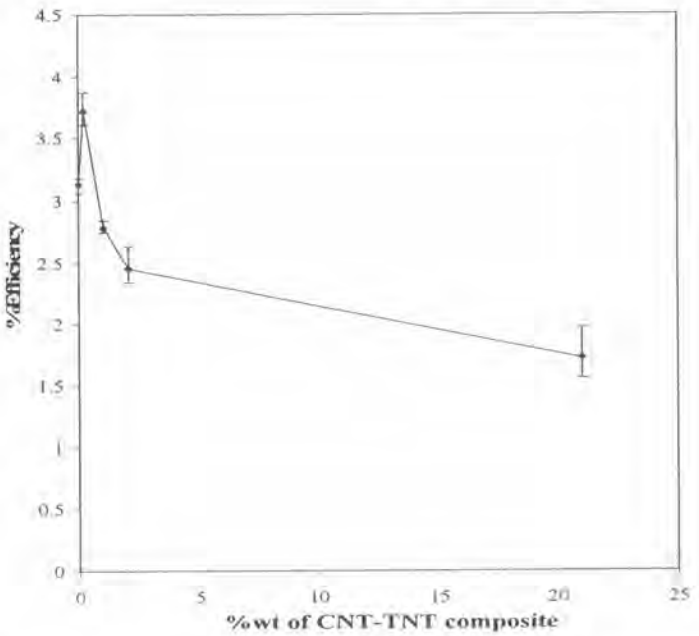

Figure 4.21 Dependence of DSSCs efficiency on amount CNT-TNT composite.

From Figure 4.21, the maximum efficiency of DSSCs containing 0.21 %wt CNT-TNT composition could be observed. Such composite could provide higher efficiency than that of TNTs additive. Not only TNTs but also CNTs play an affect on energy conversion efficiency. The presence of CNTs in the composite would increase electron transfer the electrode. However, the increase of %CNTs would oppositely lead to a decrease of the fraction of anatase powder and shielded the incident light (Lee et al., 2008). Thereby, the efficiency was dropped after adding more CNT into the composite. The similar trend could also be observed in the DSSCs containing electrodes which were made of TrCNT-TNT composite as shown in Figure 4.22.

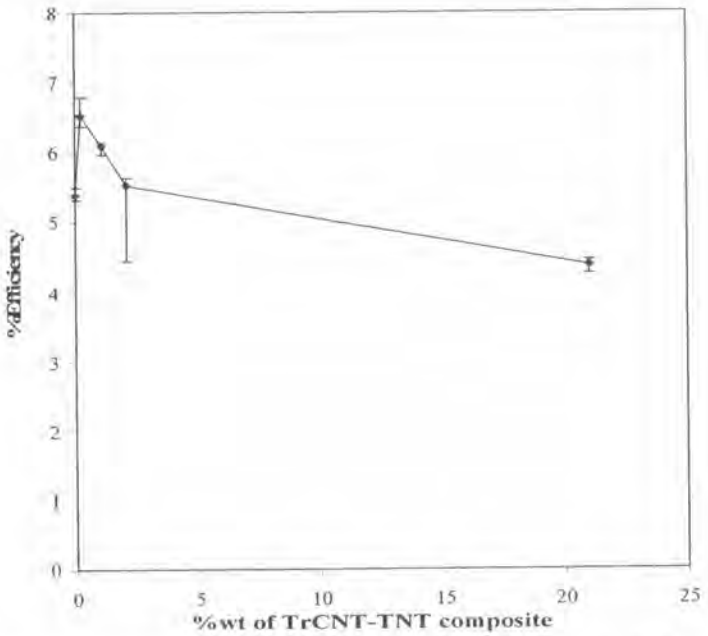

Figure 4.22 Dependence of DSSC efficiency on amount of TrCNT-TNT composite.

Referring to Figure 4.22, the efficiency raise from 5.39% to 6.53%, which is a 21.5% change. Compared with CNTs, powder of TrCNTs show the well dispersion resulted in the higher conversion efficiency. Furthermore, the effects of rice-shaped TiO_2, CNT - rice-shaped TiO_2 and TrCNT - rice-shaped TiO_2 compositions in composite materials to DSSCs were investigated, starting from rice-shaped TiO_2, shown in Figure 4.23. The efficiency was increased from 3.57% to 3.69% (3.36% increase). Although BET surface area of rice-shaped TiO_2 (ca. 80 m^2/g) was less than that of anatase TiO_2 (ca. 272 m^2/g). Rice-shaped TiO_2 could not be completely produced in the second hydrothermal process. The existence of TNTs in the rice-shaped product could effect to the efficiency of DSSCs. Compared with anatase TiO_2, the rice-shaped TiO_2 and TNTs show higher aspect ratio as ca. 5 and 80, respectively. The improve of electron transport in these DSSCs is attributed to the increase porous structure within electrode which in turn enhanced the of dye absorption.

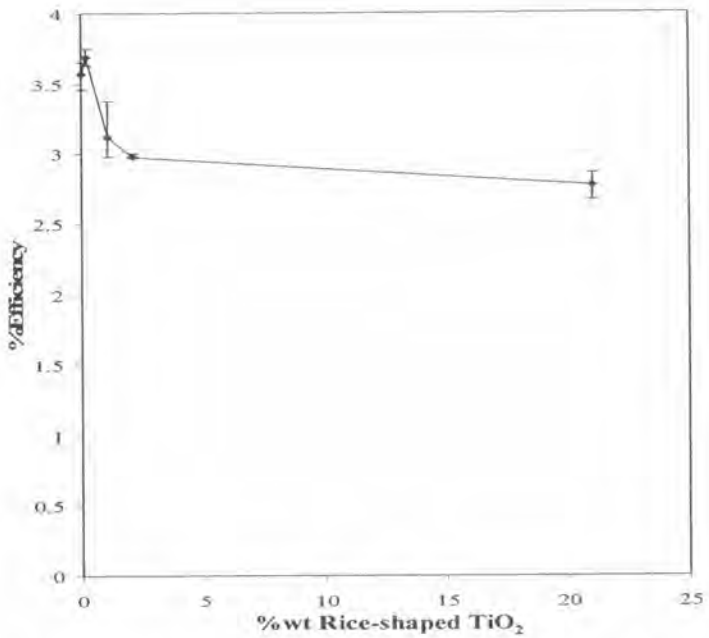

Figure 4.23 Dependence of DSSCs efficiency on amount of rice-shaped TiO_2.

The efficiencies corresponding to the amount of CNT - rice-shaped TiO_2 composite in TiO_2 film were shown in Figure 4.24. Maximum efficiency observed at the point of 0.21 %wt CNT - rice-shaped TiO_2 addition (increase from 2.64% to 2.89%). Due to the good conductivity of CNTs, the lower amount of additive increase electron transportation while the higher amount of additive increases short circuit effect.

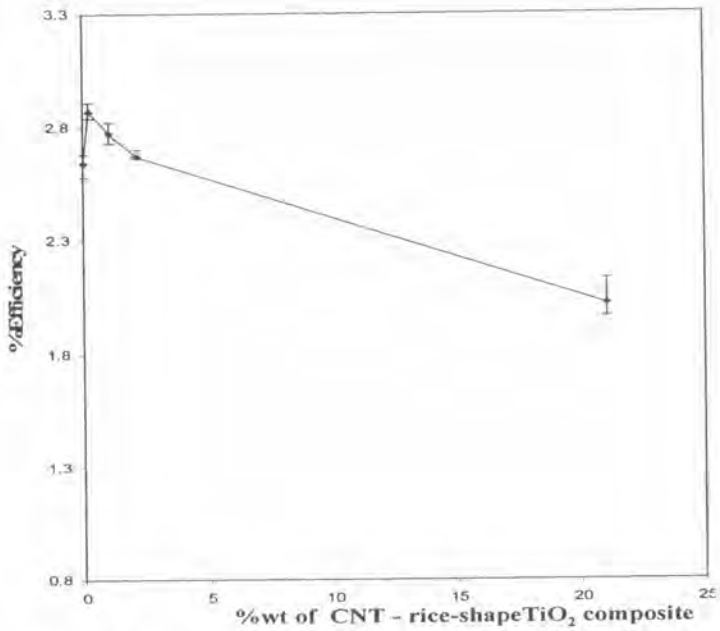

Figure 4.24 Dependence of DSSCs efficiency on amount of CNT - rice-shaped TiO_2 composite

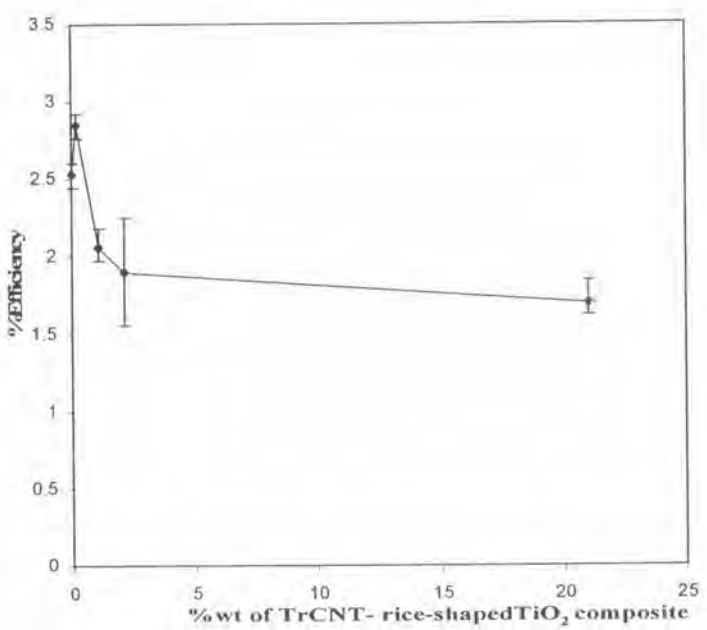

Figure 4.25 Dependence of DSSCs efficiency on amount of TrCNT - rice-shaped TiO_2 composite.

From Figure 4.25, the correlation between the amount of TrCNT - rice-shaped TiO_2 composite and efficiency of DSSCs were illustrated. The efficiency increases up to 10.98% in the presence of 0.21 %wt TrCNT – rice-shaped TiO_2 composite (from 2.55 % to 2.83%). The low addition of TrCNTs exerted their effect on electron transportation in thin film electrode. Further addition of TrCNTs may result in the shield effect of light beam incident to dye.

The film thickness is typically controlled by screen printed technique in Figures 4.26, 4.27 and 4.28. Thickness of anatase TiO_2, TNTs and rice-shaped TiO_2 film which are 9.5, 9.6 and 9.2 μm, respectively. Therefore, the dye absorption on TiO_2 electrode may not result from film thickness.

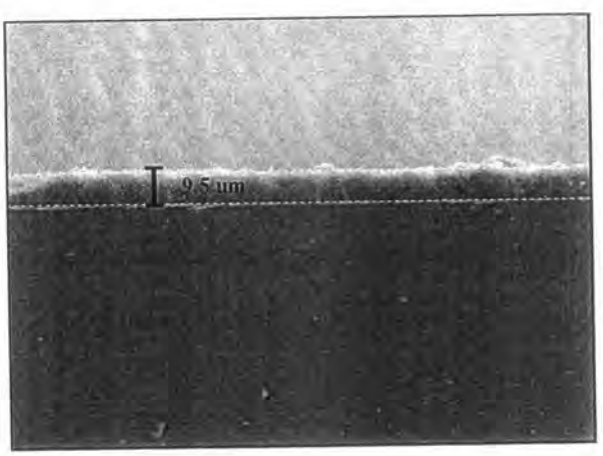

Figure 4.26 FESEM image of TiO_2 film.

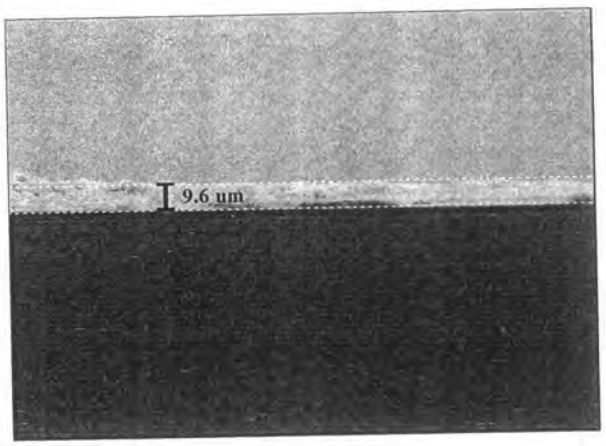

Figure 4.27 FESEM image of TiO_2 film containing 0.21 %wt TNTs.

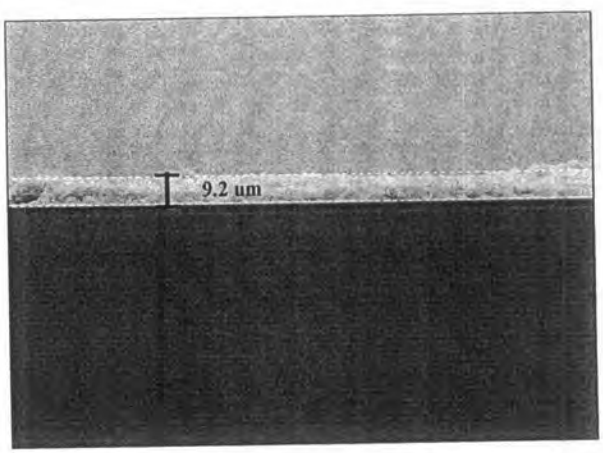

Figure 4.28 FESEM image of TiO_2 film containing 0.21 %wt rice-shaped TiO_2.

Finally, all results were concluded in Table 4.2. It could be concluded that the composite TrCNT-TNT attained the maximum of percent increasing in efficiency, compared with the others. This may result from increase of the roughness of film enhance the absorption of dye, and boost conductivity of electrode.

Table 4.2 DSSCs efficiency based on TiO_2 electrode containing various additives.

Additive	η of TiO_2 electrode(%)	η of TiO_2-additive electrode(%)	Increased efficiency(%)
TNTs	3.31	3.53	6.65
CNT-TNT	3.13	3.71	18.55
TrCNT-TNT	5.39	6.53	21.5
Rice-shaped TiO_2	3.57	3.69	3.36
CNT - rice-shaped TiO_2	2.64	2.89	8.17
TrCNT - rice-shaped TiO_2	2.55	2.89	10.98